

Note on a Floquet/Bloch-band fusion phenomenon in scattering by truncated periodic multi-well potentials

K-E Thylwe

Klöövervägen 16, 387 36 Borgholm, Sweden

(Retired from Department of Mechanics, KTH- Royal Institute of Technology)

E-mail: kethylwe@gmail.com

Abstract. A transmission phenomenon for a quantal particle scattered through a multi-well potential in one dimension is observed by means of an amplitude-phase method. The potential model consists of n identical potential cells, each containing a symmetric well. Typical transmission bands contain $n - 1$ possible energies of total transmission. It is found that certain band types contain n energies of total transmission. A fusion phenomenon of this type of band with a typical neighboring band is also found. As the transmission gap between them collapse and disappear, a resulting fused single band is seen to contain $2n - 1$ energy peaks of total transmission.

PACS numbers: 02-70.Hm, 03.65.Ge, 03.65.Nk, 03.65.-w, 31.15.-p, 73.63.-b, 81.07.St

Keywords: Hill's equation, Stability theory, Quantal transmission, Floquet/Bloch theory, Transmission bands, Amplitude-phase method

1. Introduction and presentation of results

Basic quantum physics related to truncated periodic potentials focuses on transmission and reflection properties. A free particle wave enters the potential region from one side (here from the right side); part of the wave is reflected (here in the direction $x \rightarrow +\infty$), while the remaining part of the wave is transmitted through the potential region (here in the direction $x \rightarrow -\infty$). From intensities of wave component one obtains the so-called reflection and transmission coefficients.

The present approach is similar to that for wave scattering by a single potential barrier or well [1]. A main difference in this study is that the interaction has a finite periodic structure of potential 'cells', where each cell contains a symmetric well. This part of the potential is treated as described in [2].

Quantal transmissions through multi-barrier/well systems in one dimension [3]-[12] provide important theoretical notions for analyzing tunneling in solids [13], chemical selection of gas components [14], electronic properties of material structures such as graphene [15]-[20]. Generalizations involve $2D$ models, relativistic corrections, and spin-coupling effects [21]-[26].

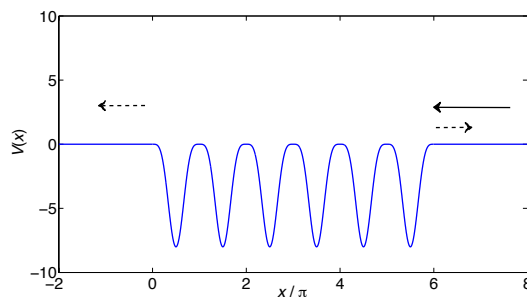


Figure 1. Illustration of a multi-well potential and traveling wave components. The incoming wave component (thick arrow) enters from the right.

Transmission effects caused by various non-vanishing exterior potentials are also in progress [27].

The truncated periodic potential is assumed vanishing outside an interval $0 \leq x \leq n\pi$, where π is the dimensionless unit length of the period (or cell) and n is the number of such cells. The potential satisfies $V(\pi) = V(0) = 0$ and its derivative with respect to x satisfies $V'(\pi) = V'(0) = 0$. The analytic form of the multi-well potential used for numerical illustrations is

$$V(x) = V_0 \sin^4(x), \quad 0 \leq x \leq n\pi, \quad V(x) = 0, \quad x < 0, x > n\pi, \quad (1)$$

where $V_0 < 0$ is the well depth. Figure 1 shows a potential with 6 identical wells in the range $0 \leq x \leq 6\pi$. Arrows indicate directions of propagating quantal waves.

The time-independent Schrödinger equation with dimensionless parameters is expressed as

$$\frac{d^2 F(x)}{dx^2} + 2[E - V(x)] F(x) = 0, \quad (2)$$

as if presented in atomic units. The symbol $E(> 0)$ represents the total scattering energy. Equation (2) is a special case of a so called Hill equation [28]-[33] for $V(x)$ in (1). Scattering boundary conditions for the wave function $F(x)$ are

$$F(x) \sim t \frac{1}{\sqrt{k}} \exp(-ikx), \quad x \rightarrow -\infty, \quad (3a)$$

$$F(x) \sim \frac{1}{\sqrt{k}} \exp(-ikx) + r \frac{1}{\sqrt{k}} \exp(ikx), \quad x \rightarrow +\infty, \quad (3b)$$

where t and r are the transmission and reflection amplitudes, respectively. The reduced (angular) wave number is

$$k = \sqrt{2E}. \quad (4)$$

The complex-valued amplitudes t and r determine the transmission and reflection coefficients from

$$T = |t|^2, \quad R = |r|^2. \quad (5)$$

The main results are presented next. Derivations by using an amplitude-phase method introduced recently in [2] are deferred to a subsequent section. Original ideas of representing a quantal wave in terms of an amplitude function and a phase function are presented in [34]-[38].

The energy dependence of the transmission coefficient within a (Floquet/Bloch) band is analyzed in some detail from an exact expression

$$T(E) = \left(1 + |\Lambda(E)|^2\right)^{-1}, \quad (6)$$

containing an imaginary quantity

$$\Lambda(E) = iJ(E) \sin n\alpha(E). \quad (7)$$

$\alpha(E)$ is the real Floquet/Bloch phase as function of energy E , an intrinsic phase defined by the wave propagation across a single cell. This phase is independent of which exact method is used. The energy dependent factor $J(E)$ is independent of n and is singular at band edges. Total transmission occurs at zeros of $\Lambda(E)$, i.e. by either of the conditions

$$J(E_J) = 0, \quad (8)$$

$$\alpha_{nj\nu} = (j + \nu/n)\pi, \quad \alpha_{nj\nu} = \alpha(E_{nj\nu}). \quad (9)$$

A band number is represented by $j = 0, 1, \dots$, and $\nu = (0), 1, \dots, n - 1$ counts the energies of total transmission within a given band. Total transmission caused by a zero of $J(E)$, for $E = E_J$, is assigned an index 'J' instead of a ν -number. $J(E)$ is not related to the much 'faster' Floquet/Bloch phase α , as function of energy. Zeros of $J(E)$ are not present in all bands. Single zeros occur in particular bands.

The case $\nu = 0$ is usually forbidden in a typical j -band. There, the phase $\alpha(E)$ is confined to an interval $j\pi \leq \alpha(E) \leq (j + 1)\pi$. Phase values $\alpha = j\pi$ and $\alpha = (j + 1)\pi$ correspond to band edges, where $J(E)$ is singular and $\sin n\alpha(E)$ is zero. Note that the product of these quantities, and $\Lambda(E)$, is still finite. If two neighboring bands, e.g. the j - and $(j + 1)$ -bands, fuse, the case $\nu = 0$ becomes valid for the $(j + 1)$ -band. Then, α is real in the larger interval $j\pi \leq \alpha(E) \leq (j + 2)\pi$. This fusion phenomenon is illustrated in figures 1 and 2.

Figure 1 shows transmission coefficients as functions of energy for $n = 6$ and three potential parameter values $V_0 = -7, -8$, and -9 . The two first bands, $j = 0, 1$, have negative energies. The top subplot ($V_0 = -7$) shows two separated transmission bands corresponding to $j = 2$ and $j = 3$. The number of energy peaks of total transmission is 5 in the band $j = 2$. Two peaks in the band $j = 3$ are less sharp. A detailed analysis shows that the peak at $E \approx 2.85$ is due to the single zero of $J(E)$. A close-lying peak at $E \approx 2.72$ is due to the phase factor $\sin n\alpha(E)$ in equation (7). There are 6 peaks of total transmission in band $j = 3$.

The bottom subplot ($V_0 = -9$) in Figure 1 shows that the band with $j = 3$ has 5 peaks of total transmission. For $j = 2$, two peaks near the band edge are unclear. A detailed analysis shows that the peak at $E \approx 1.12$ is due to the single zero of $J(E)$. A close-lying peak at $E \approx 1.32$ is due to the factor $\sin n\alpha(E)$ in equation (7). Other peaks of total transmission are due to the phase factor $\sin n\alpha(E)$.

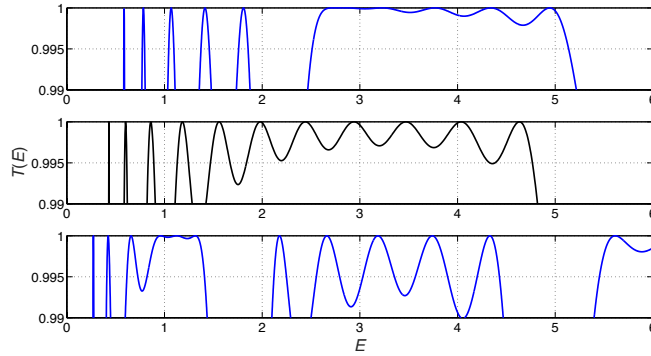


Figure 2. Energy behaviors of T for potential parameter values $V_0 = -7$ (top subplot), -8 (middle subplot), and -9 (bottom subplot). Two transmission bands with $j = 2$ and 3 are separated in the top and bottom subplots. In the middle subplot, the fused band with $j = (2, 3)$, there are 11 peaks of total transmission. Only one of two of the separated transmission bands shows 5 simple peaks of total transmission. The neighbor band has a broad peak structure which obscures the sharper peaks.

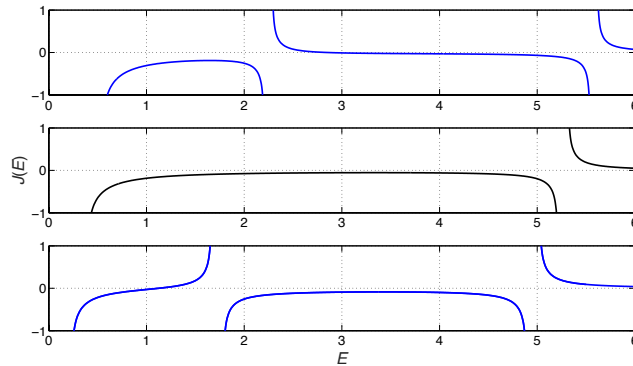


Figure 3. Energy behaviors of $J(E)$ for potential parameter values $V_0 = -7$ (top subplot), -8 (middle subplot), and -9 (bottom subplot). $J(E)$ has a zero passage near $E = 2.85$ for $j = 3$ in the top subplot, and near $E = 1.12$ for $j = 2$ in the bottom subplot. In the middle subplot, the fused band $j = (2, 3)$, $J < 0$.

In the middle subplot ($V_0 = -8$) all peaks of total transmission are due to zeros of $\sin n\alpha(E)$. $J(E)$ has no zeros. The total number of peaks is $2n - 1$. The way a gap between such bands vanishes is explained in detail in [27].

Figure 2 illustrates the energy behaviors of $J(E)$ in the complete band zones $j = 2$ and $j = 3$. $J(E)$ is imaginary in gap zones and is not illustrated. The top subplot shows that $J(E)$ has a zero and changes sign within band $j = 3$. The bottom subplot shows the same thing except that the zero occurs in band $j = 2$. The middle subplot shows the fused band, where

(n, j, ν)	$E_{n,j,\nu}(V_0 = -8)$
(6, 2, 1)	0.4310069
(6, 2, 2)	0.6020104
(6, 2, 3)	0.8594292
(6, 2, 4)	1.1829404
(6, 2, 5)	1.5592963
(6, 3, 0)	1.9804654
(6, 3, 1)	2.4414865
(6, 3, 2)	2.9392161
(6, 3, 3)	3.4715098
(6, 3, 4)	4.0368108
(6, 3, 5)	4.6336285

Table 1. Energies $E_{n,j,\nu}$ of total transmission for $V_0 = -8$.

(n, j, ν)	$E_{n,j,\nu}(V_0 = -7)$	$E_{n,j,\nu}(V_0 = -9)$
(6, 2, 1)	0.5864576	0.2720599
(6, 2, 2)	0.7839609	0.4232600
(6, 2, 3)	1.0683904	0.6575990
(6, 2, 4)	1.4144690	0.9593766
(6, 2, J)	--	1.1245588
(6, 2, 5)	1.8083837	1.3158913
(6, 3, 1)	2.7205677	2.1769876
(6, 3, J)	2.8508686	--
(6, 3, 2)	3.2275311	2.6622808
(6, 3, 3)	3.7680369	3.1848282
(6, 3, 4)	4.3405175	3.7418530
(6, 3, 5)	4.9438598	4.3311594

Table 2. Energies $E_{n,j,\nu}$ and $E_{n,j,J}$ of total transmission for $V_0 = -7$ and $V_0 = -9$. The symbol ' J ' is used for peak energies caused by $J(E)$.

$J(E) < 0$.

Energy peaks of total transmission seen in the middle subplot of Figure 1 are computed and displayed in Table 1. The fused transmission band contains $2n - 1 = 11$ such energies. Both quantum numbers, $j = 2$ and 3 , are used. The quantum number $\nu = 0$ appears for $j = 3$. All energies are due to the Floquet/Bloch phase condition in (9).

Table 2 contains energy peaks of total transmission seen in Figure 1 for the top and bottom subplots. Here, the transmission bands $j = 2$ and 3 are separated by a gap zone. Peaks of total transmission due to $J(E)$ occur. The total number of peaks for $j = 2$ and 3 is 11, the same as in Table 1, but the reasons are different.

If exterior potentials are added to the truncated potential considered, the fusion phenomenon

remains. Results of a more general investigation will be published elsewhere [27].

2. Derivations

To obtain t and r in (3a) and (3b), particular amplitude-phase solutions in each characteristic region are introduced. There are two asymptotic regions and the region of n identical cells.

Two independent solutions of (2) are defined in terms of a positive amplitude function $A(x)$ and a related real phase function $p(x)$ as [2]

$$\Psi^{(\pm)}(x) = A(x) \exp(\pm i p(x)), \quad (10)$$

$$p'(x) = A^{-2}(x) (> 0), \quad (11)$$

where $' = d/dx$. Due to the relation (11), the Wronskian determinant of the two solutions (10) is independent of x [1]. Any amplitude function satisfies a nonlinear Milne-Pinney equation [35]-[34]

$$\frac{d^2 A(x)}{dx^2} + 2[E - V(x)] A(x) = A^{-3}(x). \quad (12)$$

Amplitude functions differ by their boundary conditions [39, 40]. For any choice of $A(x)$ one has two independent exact solutions $\Psi^{(\pm)}(x)$. An amplitude function is known to be more or less oscillatory due to different choices of its boundary conditions. Several amplitude functions may be used to represent a given linear wave function. Different representations of a linear wave function can be expressed in terms of the others by linear combinations.

Equation (12) is re-written for computational purposes as a first-order differential equation as

$$\begin{bmatrix} A(x) \\ A'(x) \\ p(x) \end{bmatrix}' = \begin{bmatrix} A'(x) \\ A^{-3}(x) - 2(E - V(x))A(x) \\ A^{-2}(x) \end{bmatrix}. \quad (13)$$

The integration starts from boundary conditions of the amplitude function. The phase function needs a specified integration constant.

Amplitude-phase solutions $A(x)$ of (12) are used locally, in each characteristic region of x [39, 40]. Firstly the two exterior regions are considered. The two exterior solutions, with amplitude functions $A_L(x) = A_R(x) = k^{-1/2}$ of (12), are:

$$\Psi_L^{(\pm)}(x) = k^{-1/2} \exp(\pm i k x). \quad (14a)$$

$$\Psi_R^{(\pm)}(x) = k^{-1/2} \exp(\pm i k x) \exp(\mp i k n \pi), \quad (14b)$$

$x = 0$ and $x = n\pi$, are reference points for the respective phases. Fundamental solution matrices consist of $\Psi_{L,R}^{(\pm)}(x)$ in the upper row and $\Psi_{L,R}'^{(\pm)}(x)$ in the lower row. The exterior fundamental solutions satisfy

$$\Psi_L(0) = \begin{pmatrix} k^{-1/2} & k^{-1/2} \\ i k^{1/2} & -i k^{1/2} \end{pmatrix}, \quad \Psi_R(n\pi) = \begin{pmatrix} k^{-1/2} & k^{-1/2} \\ i k^{1/2} & -i k^{1/2} \end{pmatrix}. \quad (15)$$

In the region of the locally periodic potential it is convenient to use a real-valued fundamental solution matrix composed by the real and imaginary parts of (11). A further simplification results from the use of a periodic amplitude function $A_p(x)$. Such an amplitude function is defined by particular boundary conditions at the first cell boundary point $x = 0$, chosen as [2]

$$A_p(0) = u_p, \quad A'_p(0) = 0. \quad (16)$$

The corresponding phase satisfies $p'_p(x) = A_p^{-2}(x)$, and the phase reference point is taken at $x = 0$. Particular phase values are

$$p_p(0) = 0, \quad p_p(\pi) = \alpha; \quad p_p(n\pi) = n\alpha. \quad (17)$$

A principal fundamental solution matrix is defined by the solutions

$$S(x) = A_p(x)/u_p \sin p_p(x), \quad C(x) = A_p(x)u_p \cos p_p(x). \quad (18)$$

as

$$\Psi(x) = \begin{pmatrix} C(x) & S(x) \\ C'(x) & S'(x) \end{pmatrix}, \quad \det \Psi(x) = 1, \quad (19)$$

satisfying

$$\Psi(0) = \begin{pmatrix} 1 & 0 \\ 0 & 1 \end{pmatrix}, \quad \Psi(\pi) = \begin{pmatrix} \cos \alpha & u_p^2 \sin \alpha \\ -u_p^{-2} \sin \alpha & \cos \alpha \end{pmatrix}, \quad \Psi(n\pi) = \begin{pmatrix} \cos n\alpha & u_p^2 \sin n\alpha \\ -u_p^{-2} \sin n\alpha & \cos n\alpha \end{pmatrix}. \quad (20)$$

Note that $\Psi(n\pi) = \Psi^n(\pi)$. Calculations of u_p and α require knowledge of a single cell of the periodic part of the potential. Details of how to compute u_p and α are found in reference [2].

A connection between two fundamental solutions of the Schrödinger equation is formulated by a matrix equation involving a constant matrix. For example, the two fundamental 'exterior' solutions $\Psi_{L,R}(x)$ are related by

$$\Psi_L(x) = \Psi_R(x)\Omega, \quad (21)$$

where Ω is an x -independent matrix. Ω can be determined at any matching point, say $x = n\pi$. This gives the relation

$$\Psi_L(x) = \Psi_R(x) \left[\Psi_R^{-1}(n\pi) \Psi_L(n\pi) \right]. \quad (22)$$

The matrix value $\Psi_L(n\pi)$ can be expressed in terms of $\Psi(x)$ in (19) for the periodic part of the potential. A matching between $\Psi_L(x)$ and $\Psi(x)$ at $x = 0$ yields

$$\Psi_L(x) = \Psi(x) \left[\Psi^{-1}(0) \Psi_L(0) \right]. \quad (23)$$

By combining (22) and (23) with the use of (15) and (20), one finds the matrix Ω as

$$\Omega = \begin{pmatrix} k^{-1/2} & k^{-1/2} \\ ik^{1/2} & -ik^{1/2} \end{pmatrix}^{-1} \begin{pmatrix} \cos n\alpha & u_p^2 \sin n\alpha \\ -u_p^{-2} \sin n\alpha & \cos n\alpha \end{pmatrix} \begin{pmatrix} k^{-1/2} & k^{-1/2} \\ ik^{1/2} & -ik^{1/2} \end{pmatrix}, \quad (24)$$

i.e.

$$\Omega = \begin{pmatrix} \Delta^* & \Lambda \\ \Lambda^* & \Delta \end{pmatrix}, \quad \det \Omega = 1, \quad |\Delta|^2 = 1 + |\Lambda|^2, \quad (25)$$

with

$$\Lambda = \frac{i}{2} \left((ku_p^2)^{-1} - ku_p^2 \right) \sin n\alpha, \quad \Delta = \cos n\alpha - \frac{i}{2} \left((ku_p^2)^{-1} + ku_p^2 \right) \sin n\alpha. \quad (26)$$

The quantity Λ is expressed with the use of $J(E) = \left((ku_p^2)^{-1} - ku_p^2 \right) / 2$ in (7). With known exact elements in $\mathbf{\Omega}$, scattering boundary conditions (3a) and (3b) can be re-interpreted in terms of amplitude-phase quantities. In the left asymptotic region of x the amplitude-phase solution $\Psi_L^{(-)}(x)$ behaves as [1]

$$\Psi_L^{(-)}(x) \sim \frac{1}{\sqrt{k}} e^{-ikx}, \quad \text{as } x \rightarrow -\infty. \quad (27)$$

$\Psi_L^{(-)}(x)$ corresponds, *via* equation (21), to an equivalent expression in terms of $\Psi_R^{(\pm)}(x)$, given by

$$\Psi_L^{(-)}(x) = \Lambda \Psi_R^{(+)}(x) + \Delta \Psi_R^{(-)}(x), \quad (28)$$

where

$$\Psi_R^{\pm}(x) \sim \frac{1}{\sqrt{k}} e^{\mp ikn\pi} e^{\pm ikx}, \quad x \rightarrow +\infty. \quad (29)$$

From (28) and (29) follows

$$\Psi_L^{(-)}(x) \sim \frac{\Lambda}{\sqrt{k}} e^{-ikn\pi} e^{ikx} + \frac{\Delta}{\sqrt{k}} e^{ikn\pi} e^{-ikx}, \quad x \rightarrow +\infty. \quad (30)$$

Normalizing (30) to agree with condition (3b), the transmission and reflection amplitudes appear as

$$t = e^{-ikn\pi} \frac{1}{\Delta}, \quad r = e^{-2ikn\pi} \frac{\Lambda}{\Delta}. \quad (31)$$

The transmission and reflection coefficients defined in (5) can be expressed in terms of Λ as

$$T = \frac{1}{1 + |\Lambda|^2}, \quad R = \frac{|\Lambda|^2}{1 + |\Lambda|^2}. \quad (32)$$

This brief derivation is generalized to include exterior potentials with more general amplitude-phase methods in [27] (to be published elsewhere).

3. Concluding remarks

A formally exact amplitude-phase approach is explored in the context of one-dimensional scattering and Floquet/Bloch bands. The relevance of Floquet/Bloch theory is illustrated for a multi-well potential with $n = 6$. Band/gap structures for a given potential explains structures of transmission bands for multi-well potentials even for $n = 6$. Band types can be classified by an intrinsic quantity $J(E)$, which may have a zero or not in the band. Energy peaks of total transmission are caused by two intrinsic quantities: $J(E)$, a slowly varying functions of energy; and the intrinsic phase $\alpha(E)$, a rapidly varying function of energy.

References

- [1] K.-E. Thylwe, J. Phys. A: Math. Gen. **38** (2005) 235.
- [2] K.-E. Thylwe, Phys. Scr. 94 (2019) 065201; <https://doi.org/10.1088/1402-4896/ab40d3>.
- [3] D. J. Griffiths and C. A. Steinke, American Journal of Physics 69 (2001) 137; <https://doi.org/10.1119/1.1308266>.
- [4] M. Dharani, and C. S. Shastry, AIP Conference Proceedings 1731, 110017 (2016); <https://doi.org/10.1063/1.4948038>
- [5] Z. Shao and W. Porod, Phys. Rev. B 51 (1995) 1931.
- [6] G.-Y. Oh, arxiv.org/abs/cond-mat/9902181
- [7] F. Maiz, Physica B: Condensed Matter, 463 (2015) 93.
- [8] J. Nanda, P. K. Mahapatra, C. L. Roy, Physica B: Physics of Condensed Matter, Vol.383(2) (2006) 232
- [9] S. Mukhopadhyay, R. Biswas, C. Sinha, Physics Letters A, Vol.376(15) (2012) 1306.
- [10] K. W. Yu, Computers in Physics 4, 176 (1990), <https://doi.org/10.1063/1.168361>.
- [11] D. W. L. Sprung, Hua Wu, and J. Martorell, American Journal of Physics 61 (1993) 1118, <https://doi.org/10.1119/1.17306>.
- [12] D. Bar, International Journal of Theoretical Physics, Vol. 44, (2005) 1281, DOI: 10.1007/s10773-005-4686-x
- [13] C. B. Duke, *Tunneling in Solids* (Academic, New York and London, 1969).
- [14] S. Mandrà, J. Schrier, M. Ceotto, The journal of physical chemistry. A, Vol.118(33) (2014) 6457.
- [15] M. Dragomana, D. Dragoman, Progress in Quantum Electronics 33 (2009) 165214; A. H. Castro Neto, F. Guinea, N. M. R. Peres, K. S. Novoselov and A. K. Geim, Rev. Mod. Phys. 81 (2009) 10962.
- [16] A. Zubarev and D. Dragoman, Physica E 44 (2012) 1687.; A. Zubarev and D. Dragoman, J. Phys. D: Appl. Phys. 47 (2014) 425302.
- [17] D. S. Daz-Guerrero, L. M. Gaggero-Sager, I. Rodriguez-Vargas and O. Sotolongo-Costa, Panchadhyayee, Pradipta Philosophical Magazine, (2013) 1.
- [18] L. A. Cury, N. Studart, Superlattices and Microstructures, Vol.4(2) (1988) 245.
- [19] G. Karavaev, N. Chuprikov, Russian Physics Journal, Vol.36(8) (1993) 749.
- [20] S. Kumar; S. Kumari Int. J. of Nanoparticles, Vol 10 (2018) 92.
- [21] P. Pyykkö, Chem. Rev. 88 (1988) 563.
- [22] P. Pereyra, J. Phys. A 31 (1998) 4521 .
- [23] Siddhant Das, American Journal of Physics 83 (2015) 590; <https://doi.org/10.1119/1.4916834>.
- [24] R. Zhao, Y. Zhang, Y. Xiao, and W. Liu, J. Chem. Phys. 144 (2016) 044105.
- [25] C L Roy, Journal of Physics: Condensed Matter, Vol.5(41) (1993) 7701.
- [26] C.H. Chen, P. Tseng, W.J. Hsueh, Physics Letters A 380 (2016) 2957.
- [27] K.-E. Thylwe, <http://arxiv.org/pdf/2005.11695>.
- [28] W. Magnus and S. Winkler 1979 *Hill's Equation* (Dover, New York).
- [29] F. Bloch, Z. Phys. 52 (1929) 555-600.
- [30] R. Grimshaw 1990 *Nonlinear Ordinary Differential Equations*. Applied Mathematics and Engineering Science Texts, Oxford: Blackwell.10: 0632027088
- [31] C. Kittel, 1996 *Introduction to Solid-State Physics*, 7th edition (John-Wiley, Singapore) pp. 173-196.
- [32] J. Kevorkian and J. Cole 1981 *Perturbation Methods in applied Mathematics*. Berlin: Springer-Verlag.
- [33] C. Hayashi 1964 *Nonlinear Oscillations in Physical Systems*. New York: McGraw-Hill.
- [34] E. Pinney, Proc. Am. Math. Soc. 1 (1950) 681.
- [35] W. E. Milne, Phys. Rev. **35** (1930) 863.
- [36] J. A. Wheeler, Phys. Rev. 52 (1937) 1123.
- [37] Wilson H A 1930, *Phys. Rev.* **35**, 948.
- [38] Young H A 1931, *Phys. Rev.* **38**, 1612.; Young H A 1932, *Phys. Rev.* **39**, 455.
- [39] K.-E. Thylwe, J. Math. Chem. **53**, (2015) 1608.; K.-E Thylwe, Phys. Scr. **85** (2012) 065009.
- [40] K.-E. Thylwe, J Math Chem 56 (2018) 2674.